14th IMEKO TC10 Workshop Technical Diagnostics
New Perspectives in Measurements, Tools and Techniques
for system's reliability, maintainability and safety
Milan, Italy, June 27-28, 2016

Surface quality monitoring in micromilling: a preliminary investigation on microfeatures

Paolo Parenti[1], Marco Camagni[1], Massimiliano Annoni[1]

[1] *Politecnico di Milano, via La Masa 1, 20156, Milano*

Abstract – Process monitoring plays a key role in industrial machining operations such as turning, milling and grinding, for assuring part quality and long lifespan of cutting tools to reduce production costs. When the part dimensions are scaled down to submillimeter range, process monitoring becomes essential but harder to implement. This work evaluates the possibility to monitor the surface quality of micromilled parts by means of cutting-related signals, such as Cutting Forces and Acoustic Emission. Micromilling of cylindrical pins with 0.8 mm diameter and aspect ratio of 1.875 has been studied, representing a significant case for injection molds. This manufacturing task is challenging because both the dimensional/geometrical accuracy and the finishing quality of the part have to be maximized to guarantee the final part functionalities. On the other side, the direct measurement of these characteristics on the final parts is challenging considering the state-of-the-art metrology systems. This fact motivates the adoption of indirect monitoring approaches, that can estimate the part quality in alternative ways. A design of experiment approach (DoE) together with Analysis of Variance (ANOVA), have been adopted to assess the statistical relationship between the monitored signals and the quality indexes of interest, such as the average surface roughness of the parts. The emerged correlations between the achievable surface roughness and process parameters, together with the existing correlation of micro cutting forces and acoustic emission with process parameters, sustain the feasibility of using these signals for implementing advanced monitoring and control schemes of the micro cutting operation.

Keywords: **Micromilling, Acoustic Emission, Cutting Forces, Monitoring, ANOVA, Surface texture**

1. INTRODUCTION

Part quality in micromilling is more difficult to control compared to macro cutting processes due to numerous phenomena that rise up during cutting operations. The most significant differences consist in the strong ploughing that govern micro cutting and in the lower static stiffness of the milling tools and parts caused by their low dimensions. When considering micro features as cylindrical pins used as mold cores, two important quality factors are required to improve the mold performance i.e. a strict dimensional/geometrical accuracy and an appropriate surface finishing. While most of the dimensional/geometrical accuracy constraints can nowadays be fulfilled by the adoption of extremely accurate micromilling machines and spindles, the surface texture generation is still an open issue in machining and especially in micromilling. Two approaches can be used to predict the texture characteristics: theoretical and experimental. From the former point of view, researchers are developing models to support the arising need to control the micromilled surface texture by means of the milling parameters selection. An example of the theoretical approach is the dynamic model [1] that links the generated texture and the cutting forces in micromilling for manufacturing micro-molds. Vehmeier [2] presented another surface generation model able to control the basic mechanism of surface generation and simulate the topography of micromilling, with defined cutting edges geometry. The biggest problem of the theoretical approaches is the lack of generality with respect to the variation in material and microstructure characteristics, tool shapes and toolpaths and their inability to describe real phenomena such as tool wear, chip adhesion etc. On the other side, predicting and monitoring in a robust way the achievable roughness in real industrial cases can be done by applying a strong experimental approach based on surface topography measurements, as done in micromilling cases in [3],[4]. Most of the experimental approaches attempt to derive a link between the machining parameters, as the feed, the tool orientation and the 3D topographies. Literature confirms that the machining parameters mainly affecting the different texture generation in micromilling are depth of cut, feed per tooth, milling strategy and spindle speed [5]. When the machined features become more complex, such as when aspect ratios increase (and static stiffness decreases) as for the studied cylindrical pins, dedicated investigations are required to understand the phenomena involved in the texture generation, with the aim to better monitor and control the cutting process. Even if many machining studies already used Cutting Forces and Acoustic Emission signals to monitor machining operations [6],[7],[8], no studies seem currently available on micromilled pin texture monitoring, where limited stiffness affects both part and mill.

A previous study by the present paper authors [9] identified the presence of a direct relationship between process parameters and workpiece quality in case of thin wall manufacturing and pointed out the process parameters effect on cutting forces [10].

This study performs a similar investigation basing on the acquisition of Forces and Acoustic Emission signals in cylindrical thin pins with the aim to improve their surface finish. Section 2 describes the test case and the experimental setup involving both the manufacturing cycle and the measurement procedures. A presentation on the achieved results, which focuses on outlining the relationship between surface roughness, cutting parameters and acquired monitored signals, then follows in Section 3.

2. MATERIAL AND METHODS

The present study target feature is a pin with diameter of 800 µm and height of 1.5 mm, made of AISI420 (UNI X20Cr13). The material has been selected as representative of molds applications where, for instance, core pins roughness has to be minimized to reduce extraction forces during the micro-injection molding process. In order to represent a pin array configuration, characterized by limited pin centre-to-centre distance, playing a role on the cutting process, the machined samples contain multiple pins closely positioned side by side (Figure 1). In the study, different pins have been realized with different machining parameters and forces and acoustic emissions were acquired during cutting operations. Synthetic indicators were then extracted from those signals and were compared to the actual surface roughness, directly measured on pins surface.

Experimental Setup/Design

A Kern EVO ultra precision 5-axis machining centre has been used in 3-axis configuration to machine the studied pins (Figure 1). Workpiece is firstly roughed by using a CAM software (CimatronE®) generated toolpath. Then, it has been finished in dry conditions, according to the required experimental plan parameters (Table 2). Two-Flute Coated Carbide Flat End Mills (Code: HLS 2005-020), with 0.5 mm of diameter, 30° helix angle and 0.7 mm of maximum axial depth of cut from Union Tool have been used for finishing. A down-milling Z-Plane approach is adopted in order to limit tool wear and tool passes overlapping that would generate less replicable cutting conditions. In addition, since tool wear was not the object of the study, multiple tool units were adopted in the experimentation. All the adopted milling tools were presetted by using an on-board optical presetting system (Marposs VTS©) that is able to measure the tool in running conditions.

A proper factorial experimental design (2^3 factorial, replicated three times, fully randomized) has been prepared in order to point out the effects of the selected process parameters on the cutting forces and on the pin geometrical quality characteristics. The selected factors levels have been determined in a preliminary experimental campaign based on mill manufacturer suggested guidelines and on previous authors experience (Table 2).

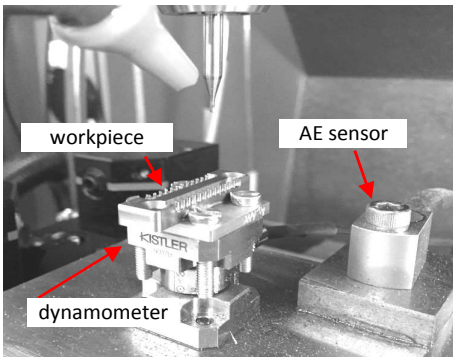

Figure 1. Experimental setup on the machine

Force and Acoustic Emission measurements

A top piezoelectric load cell (Kistler 9317B) was used to measure cutting forces. The triaxial cell was amplified by three Kistler 5015A charge amplifiers. Signals were acquired by a National Instrument USB 9234 board at a 51.2 KHz sampling frequency.

Table 2. Experimental design summary

Factor	Symbol	Levels
Axial depth of cut	ap [µm]	700
Radial depth of cut	ae [µm]	10, 20
Feed per tooth	fz [µm]	6, 12
Revolution speed	*N* [rpm]	24000, 32000

Cutting force measurements were affected by vibrations, due to the low resonance frequency of the fixturing and force measurement system, excited by the Tooth Passing Frequency (TPF) multiple harmonics. The main resonance was approximately 4000 Hz in both *X* and *Y* directions. The Frequency Response Functions (FRF) resulting from an impact test on the fixturing and force measurement system was identified and used to compensate the measures.

Since the tool moves around the pin following a circular trajectory in this study, it has been decided to analyze the Resultant Cutting Force *FR*, computed from the acquired forces in *X-Y-Z* directions. However, the vertical force component *Fz* was negligible in all the cases. As can be noticed in Figure 2 (depicting Test #2 with a_e =20 µm; f_z = 6 µm; *N* = 32000 rpm), *FR* is characterized by the typical pulsing profile of a milling operation. In the showed case, as in all the other tests, the first cutting harmonic (Tooth Passing Frequency, (TPF), in the picture at 32000/60*2 = 1066 Hz) is the spectrum highest component, followed by the spindle frequency (at

32000/60 = 533 Hz), which is caused by tool and spindle run-out.

On the other side, a Kistler 8152B221 AE sensor is adopted for the acquisition of the Acoustic Emission signals, generated by the cutting process. In particular, the RMS computed at 0.0001 s by the conditioning board, has been acquired at 51.2 KHz. One of the advantages of the use of AE for process monitoring consists in the fact that the sensor frequency bandwidth (~ 0.5 MHz) is much higher than machine vibrations and ambient acoustic noise.

Surface texture measurements

The workpiece measurements have been performed by a 3D white light interferometer (Bruker Countour Elite™ K [11]). Almost half of the pins lateral surfaces were measured for all the pin length by adopting multiple images stitching acquisitions.

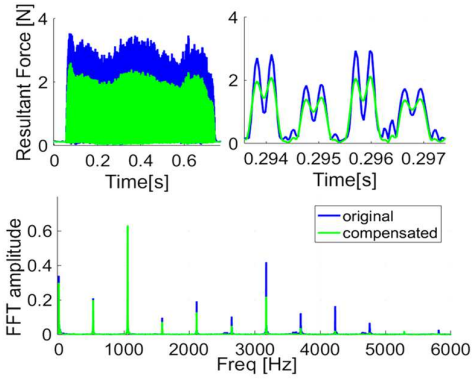

Figure 2. Resultant Cutting Force FR during Test #2

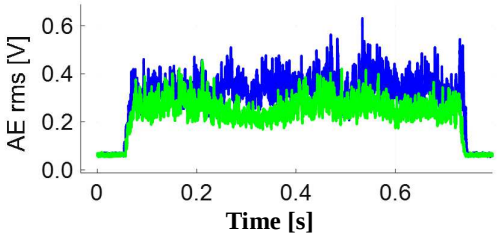

Figure 3. AE RMS signals during Test #2

After the acquisition of the Dataset, a Data Restore and a user designed Masking and Filtering were applied to compute the areal texture parameter on the central area, Figure 4. In addition, a peak removal function was applied to eliminate some optical artifact peaks that affected the data. Texture has been evaluated in terms of surface vertical (i.e. Height) deviations respect to the ideal one by means of the Surface Arithmetical Mean indicator *Sa*, which is one of the most widespread areal surface roughness parameters [12]. The arithmetic mean height *Sa* is defined as the arithmetic mean of the absolute value of the height within a sampling area (Eq.1).

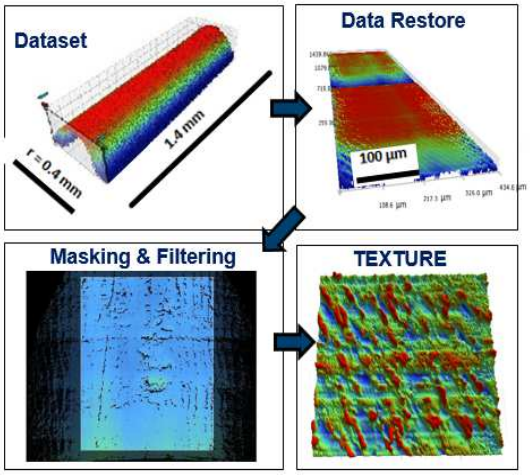

Figure 4. Texture measuring and filtering procedure

$$S_a = \frac{1}{A}\iint_A |z(x,y)|\,dx\,dy \qquad (Eq.1)$$

3. RESULT AND DISCUSSION

The tests were carried out according to the designed plan (Table 2). Three different milling tools were used to machine the 24 pins. The tool measurements after each test confirmed that tool wear was negligible.

Most of the surfaces showed a basic regular pattern with inclined marks created by the conjunct effect of mill helix angle and feed. Relatively large ploughing marks were visible in the conditions with smaller *ae* and few scratches were randomly distributed on the pin surfaces. Figure 5 depicts both Test #2 and Test #20 (a_e =10 µm; f_z = 6 µm; *N* = 32000 rpm), respectively.

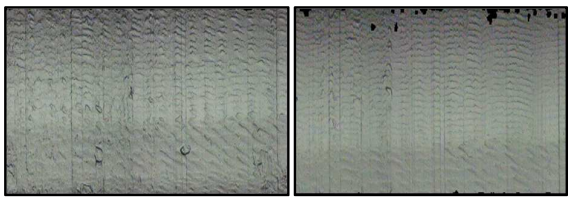

Figure 5. Finished pin surfaces of Test #2 and #20

The first ANOVA result is that the rotational speed *N* is not significant on *Sa* (Table 3). Consequently, the attention has to be given to the two factors *ae* and *fz*, whose main effects (*ae*, *fz*) and interaction (*ae***fz*) played a role on the *Sa* parameter. The biggest effect is played by *ae*, whose higher levels lead to average worst roughness values, around Ra ≅ 320 nm. The limited effect of the feed per tooth compared to the radial depth of cut cannot be easily predicted by using standard kinematic analysis of the cutting process, as discussed in literature. In micromilling in fact, the phenomenon of minimum chip thickness generates a continuous alternation of the ploughing-dominated and shearing-dominated cutting zones, playing

a dominant role in the cutting surface generation, where ploughed marks can lead to an increase of the overall roughness.

Table 3. ANOVA Table "Sa versus ae; N; fz"

Source	DF	Adj SS	Adj MS	F-Value	P-Value
ae	1	32801	32801	34.61	0.000
N	1	217.3	217.3	0.23	0.639
fz	1	2286.2	2286.2	2.41	0.14
*ae*N*	1	89.3	89.3	0.09	0.763
*ae*fz*	1	3543.6	3543.6	3.74	0.071
*N*fz*	1	5164	516.4	0.54	0.471
*ae*N*fz*	1	1582	1582	1.67	0.215
Error	16	15165.4	947.8		
Total	23	56201.2			

On one side, this phenomenon can be limited by adopting bigger maximum chip thicknesses, i.e. feeds per tooth: in effects, higher feeds per tooth lead to a decrease of surface roughness in this study (Figure 8). On the other side, the use of a big axial depth of cut *ap* (Table 2) could have introduced a high sensitivity of the surface roughness to the *ae* parameter, due to the relatively large radial deflection that could have affected the system due to the cutting forces. In effects, this possible explanation agrees with the fact that the feed per tooth seems to play a stronger effect when *ae* is bigger (Figure 6).

It is now interesting to analyze how the acquired signals relate to the cutting parameters. Regarding the force signal, the RMS of the Resultant Cutting Force ranges between 0.6 and 1.25 N. The overall variability inside the three replicates seems very small. The significant factors are illustrated in Table 4, where a P-value less than 0.05 indicates statistical significance.

Again, the strongest effect is played by the radial depth of cut *ae*, both as direct effect and interactions with the other parameters.

A bigger *ae* always causes an increase of the force RMS and this fact was expected since the contact time increases with *ae*, as a consequence of the bigger angular tool engagement. Indeed, the spindle speed *N* is not a significant factor alone, but it becomes significant as interactions with both the other parameters. It can be noted that the feed per tooth *fz* is very significant and its increase causes an increase in the forces. Eventually, it is interesting to note that the interaction *ae*fz*N* is the MRR, i.e. the nominal cutting Material Removal Rate, Its statistical significance is somehow in agreement with the cutting modelling theory that foresees an increase of the cutting force when MRR increases [1].

Looking at the Figure 8 that depicts the scatterplot between the surface roughness *Sa* [nm] and the Resultant Force *FR* [N], it can be noticed that a (weak) correlation between the *Sa* and the cutting forces seems to exist. The effect of *ae*, which deteriorates the surface roughness, is well captured by the *FR* force, that increases rapidly, passing from the smaller to the bigger *ae* value. This fact is true even considering the opposite effect of the feed per tooth that, on one side decreases the surface roughness but, on the other side, increases the forces.

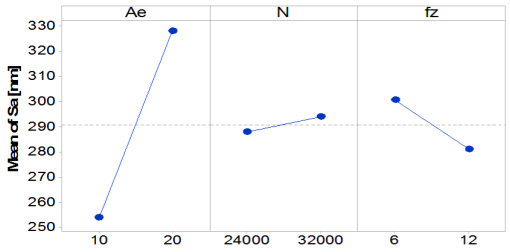

Figure 6. Main Effect plots for Sa

Table 4. ANOVA Table "FR (Resultant Cutting Force) versus ae; N; fz"

Source	DF	Adj SS	Adj MS	F-Value	P-Value
ae	*1*	*1.03609*	*1.03609*	*3698.93*	*0.000*
N	*1*	0.00007	0.00007	0.25	0.622
fz	*1*	0.08975	0.08975	320.40	0.000
*ae*N*	1	0.00016	0.00016	0.57	0.463
*ae*fz*	1	0.00574	0.00574	20.48	0.000
*N*fz*	1	0.00027	0.00027	0.95	0.344
*ae*N*fz*	1	0.02893	0.02893	103.28	0.000
Error	15	0.00420	0.00028		
Total	22	1.22902			

This information can be exploited for controlling the process e.g. through a signal threshold for triggering process control actions.

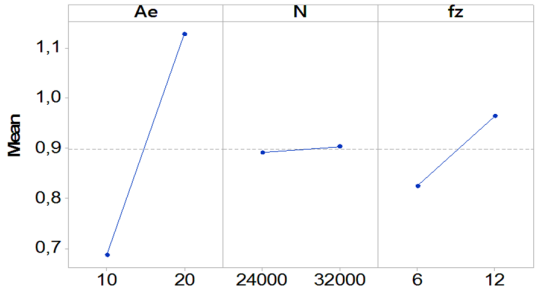

Figure 7. Individual value and Main Effect, for the Resultant Cutting Force FR

Let us consider now the Acoustic Emission signal. During the chip removal process, Acoustic Emission generates in the form of transient elastic waves propagating in the structure. As discussed, different causes make the AE signal rise, as the material plastic and elastic deformation and the chip formation phenomena, like friction (mainly between the chip and tool rake face and between the tool flank and the workpiece material), chip adhesion, breakage and collision with the cutting tool. Moreover, the AE signal is a function of the sensor setup since it also captures the elastic waves reflections influenced by the material density and geometrical

discontinuities on the path between the process and sensor points.

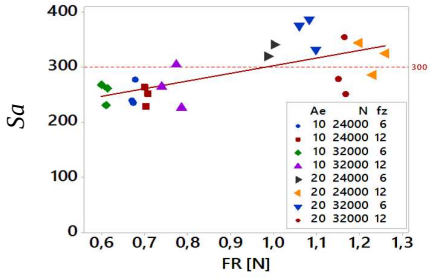

Figure 8. Scatterplots of Sa versus FR

The present study confirmed the expected sensitivity of the AE sensor in respect to the cutting operation, despite the sensor position was not extremely close to the cutting contact point due to the limitations caused by sensor dimensions (Figure 1). Figure 3 depicts the AE RMS signal for two different cases with different radial immersion *ae* = 20 µm and 10 µm, respectively. It can be observed that the signal to noise ratio increases when cutting begins, at around 0.05 s from the beginning of the acquisition. The signals in the two cases show a different mean value but also a different variability, governed by the presence of randomly distributed peaks. Since all the AE RMS signals present a very dense spectral energy, it has been decided to take into account, besides the pure AE RMS mean value, also a narrow band competing to the first cutting frequency of the AE RMS spectrum. It is expected that this frequency band contains more process kinematic information and therefore more information related to the surface texture generation.

The two AE RMS synthetic indicators, i.e. the AE RMS mean and the AE RMS peak at the TPF, seem not related to each other (Figure 9), but the ANOVA confirms that the three main process parameters affect both of them (and that none of the parameters interaction is statistically significant). It is interesting to note, by looking at the main effect plot in Figure 9, that the spindle speed plays an opposite role on the two indicators: increasing *N* produces an increase of the AE RMS mean and, at the same time, a decrease of the AE RMS TPF amplitude peak. It is not clear why this fact happens and further investigations have to be carried out to clarify this evidence. However, both the AE RMS indicators show a direct proportionality with *ae* and an inverse proportionality with *fz*. This result does not seem in agreement with the expected proportionality between the AE RMS mean and the MRR already found by other authors [6]. Now, the point is to check whether a relationship between the AE RMS and the surface roughness *Sa* exists.

The direct correlation between the AE RMS indicators and *Sa* is not clear, as showed in Figure 10: in both cases, there is not a clear connection between the indicators and the *Sa* value.

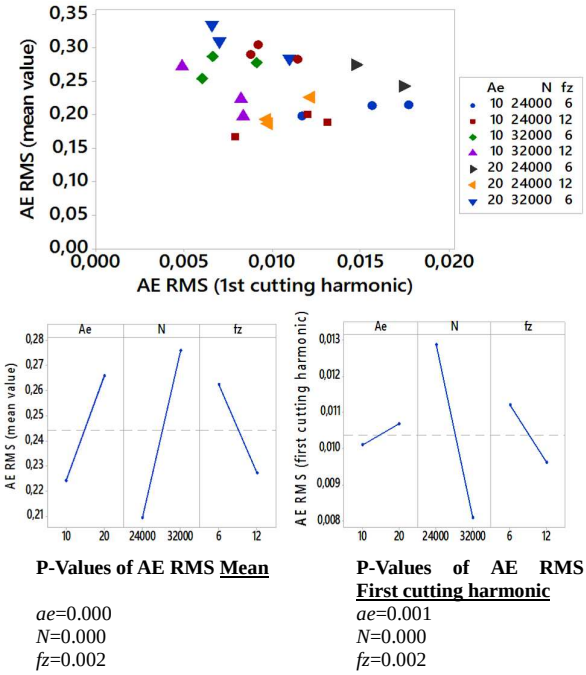

P-Values of AE RMS Mean

ae=0.000
N=0.000
fz=0.002

P-Values of AE RMS First cutting harmonic

ae=0.001
N=0.000
fz=0.002

Figure 9. Scatter and Main Effect Plots of the AE RMS mean value and AE RMS TPF

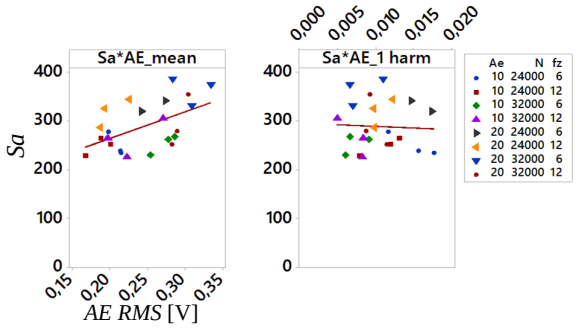

Figure 10. Scatterplots of Sa vs. AE RMS mean value and AE RMS TPF

For this reason, the use of the AE RMS as a signal for implementing a *Sa* monitoring and control system is neither obvious, nor trivial. Without a model describing the relationship between AE and process parameters, it is therefore impossible to exploit the information contained in the AE signal as a feasible information source for process monitoring and control systems.

4. CONCLUSIONS

In this paper, the surface generation in micromilled cylindrical features has been investigated. The effect of the main cutting parameters on the achieved surface arithmetic mean height *Sa* has been pointed out, through a suitable experimental campaign. It has been found that the radial depth of cut is the main parameter affecting the surface

generation, followed by the feed per tooth. The optimal parameter combination for minimizing the roughness resulted the highest feed per tooth, the lowest cutting speed and the lowest radial depth of cut. The relationship existing between the process parameters and the monitoring signals (Resultant Cutting Force and Acoustic Emission) has also been pointed out for supporting the adoption of the corresponding sensors in process monitoring and control approaches. The Resultant Cutting Force seems promising under this point of view, while Acoustic Emission needs further investigations.

This study then represents a step towards a sensor-based online quality monitoring and control system.

Real time control systems could be implemented basing their decisions on signals that are easily measurable in the process as cutting forces and acoustic emission.

Being the adopted *Sa* surface quality index quite insensitive to the distribution of peaks, valleys and spacing of the various texture features, it is not capable to capture the entire process fingerprint information. Therefore, the link between the monitoring signals and the surface could be verified also in respect to other surface texture indicators that address more specific surface details.

Moreover, this research could be extended by investigating the capacity of the studied signals to support the analysis of the geometrical/dimensional part deviations and burr formation, which are other fundamental aspects for micro milling processes.

5. ACKNOLEDGEMENT

The authors are very grateful to Francesco Biancardi and Samuel Lesko from Bruker Nano Surfaces Division for their support with the adopted optical interferometric microscope.

6. REFERENCES

[1] P. Kurczewski, J. Vehmeyer, J. C. Outerio, Simulation Model for Micro-Milling Operations and Surface Generation, Vol. 223, Health Press, 2011, pp. 849–858.

[2] J. Vehmeyer, S. Hinduja, L. Li, A surface generation model for micro cutting processes with geometrically defined cutting edges, Springer London, 2013, pp. 149–152

[3] H. Liu, Y. Sun, Y. Geng, D. Shan, Experimental research of milling force and surface quality for tc4 titanium alloy of micro-milling, The International Journal of Advanced Manufacturing Technology 79 (1-4) (2015) 705–716.

[4] G. Kiswanto, D. L. Zariatin, T. J. Ko, The effect of spindle speed, feed-rate and machining time to the surface roughness and burr formation of aluminum alloy 1100 in micro-milling operation, Journal of manufacturing processes 16 (4) (2014) 435–450.

[5] P. G. Benardos, G. C. Vosniakos, Predicting surface roughness in machining: a review, International journal of machine tools & manufacture 43 (8) (2003) 833–844.

[6] Thepsonthi, T., & Özel, T. (2010). Sensor-Assisted Monitoring and Optimization of Process Parameters in Micro-end Milling of Ti-6Al-4V Titanium Alloy Milling, 227–235.

[7] Tansel, I., Trujillo, M., Nedbouyan, a, Velez, C., Bao, W.-Y., Arkan, T. ., & Tansel, B. (1998). Micro-end-milling—III. Wear estimation and tool breakage detection using acoustic emission signals. International Journal of Machine Tools and Manufacture, 38, 1449–1466. doi:10.1016/S0890-6955(98)00017-0

[8] Zhang, S. J., To, S., Zhang, G. Q., & Zhu, Z. W. (2015). A review of machine-tool vibration and its influence upon surface generation in ultra-precision machining. International Journal of Machine Tools and Manufacture, 91, 34–42. doi:10.1016/j.ijmachtools.2015.01.005.

[9] M. Annoni, S. Petrò, L. Rebaioli, Q. Semeraro, R. Solito, 2012, Thin wall geometrical quality improvement in micromilling , The International Journal of Advanced Manufacturing Technology, July 2015, Volume 79, Issue 5, pp 881-895

[10] M. Annoni, S. Petrò, L. Rebaioli, Q. Semeraro, R. Solito, Process parameters effect on cutting forces and geometrical quality in thin wall micromilling, Proceedings of NAMRI/SME, Vol. 41, 2013

[11] Bruker contour GT specification, https://www.bruker.com

[12] Iso 25178-2: Geometrical product specifications (gps) - surface texture: Areal. part 2: Terms, definitions and surface texture parameters, international organization for standardization, Geneva, Switzerland.